Dependence of the photoionization cross-section of α-Al$_2$O$_3$:C on the measurement temperature

A. Nyirenda, M.L. Chithambo

Department of Physics and Electronics, Rhodes University, P.O Box 94, Grahamstown 6140, South Africa

E-mail: `anyirenda@gmail.com`

Abstract. We report the temperature dependence of the photoionization cross-section, that is, the effective area of interaction between incident photons and charge trapping states in α-Al$_2$O$_3$:C, a highly sensitive dosimetric material. Samples were exposed to 1.0 Gy of beta irradiation followed by measurement of linearly-modulated optically stimulated luminescence under 470 nm blue LED stimulation. The technique involves the linear increase of the power of stimulating signal from a minimum to some maximum value for which the luminescence appears as a spectrum of overlapping time-dependent peaks. The apparently single peak comprises of at least two components henceforth referred to as fast and slow components as determined by analytical deconvolution of the original spectrum. The position of each of the component peaks shifts to earlier times with increasing measurement temperature. In addition, the photoionization cross-section for both fast and slow components increases, due to increased electron-phonon coupling, from $(1.18 - 1.33) \times 10^{-18}$ cm^{-2} and $(4.05 - 5.22) \times 10^{-19}$ cm^{-2} respectively as measurement temperature increases from 30°C to 100°C.

1. Introduction

α-Al$_2$O$_3$:C is highly sensitive to ionizing radiation and is currently used for thermoluminescence and optically stimulated luminescence (TL/OSL) dosimetry specifically for personal and environmental monitoring. Thermoluminescence (TL) is a stimulated luminescence phenomenon which involves a non-isothermal scan of a pre-irradiated luminescent material to produce a spectrum of one or more temperature resolved peaks in luminescence intensity known as a 'glow-curve'. A TL peak is associated with the presence of certain species of point defects which may act as electron or hole traps during excitation of the material by an external energy source e.g. ionizing radiation. When the stimulating energy is optical in nature, the phenomenon is referred to as optically stimulated luminescence (OSL). OSL methods of dosimetry are preferred to TL methods since the former enable multiple read-outs of the OSL signal unlike the latter.

Linearly modulated optical stimulation of luminescence (LM-OSL) is an OSL method used for probing luminescence materials. In LM-OSL, the stimulating power from the light source is linearly increased from a minimum to some maximum value while monitoring the OSL throughout the whole stimulation period. The resulting OSL spectrum appears as a series of peaks with each one representing a component of the OSL signal with particular photoionisation cross-section [1]. The photoionisation cross-section is perhaps the most important parameter that governs trap ionisation and dictates the stability of a particular trap during optical stimulation [2]. It follows that at a particular stimulating wavelength, an electron trap with

a relatively large photoionisation cross-section will empty quickly and produce peaks at earlier times in the resultant curve. Thus, the LM-OSL signal allows more effective and accurate characterisation of each OSL component [1].

For first order kinetics i.e. negligible charge recapture at a trap following stimulation, the instantaneous LM-OSL intensity, $L(t)$, is given by the following equation:

$$L(t) = \gamma\; t\; \Sigma_i\; n0_i\; p_i \exp\left(-\frac{\gamma\; p_i\; t^2}{2}\right);\; \gamma = T_{stim}^{-1} \tag{1}$$

where γ is the stimulation power ramping rate, T_{stim} is the total stimulation time, $n0_i$ is the initial trapped charge population in the ith trap is the detrapping probability, t is time in seconds. The summation is carried over all the component peaks [2]. The photoionization cross-section, σ_i, is obtained from the detrapping probability by using the relationship

$$p_i = \sigma_i\; \Phi \tag{2}$$

where Φ is the maximum stimulation photon flux. The maximum stimulation photon flux is calculated as

$$\Phi = \frac{maximum\; power\; density}{energy\; per\; photon} \tag{3}$$

where the energy per photon is hc/λ and h is the Planck's constant, c is the speed of light in vacuum. For blue LEDs ($\lambda = 470$ nm) with a maximum power density of 80 mWcm^{-2} at sample position, $\Phi = 1.89 \times 10^{17}$cm^{-2} s^{-1}.

The peak position, $t_{max,i}$, is given by

$$t_{max,i} = \sqrt{\frac{1}{p_i\; \gamma}} = \sqrt{\frac{T_{stim}}{\sigma_i\; \Phi}} \tag{4}$$

In cases where charge retrapping during optical stimulation is significant i.e. general order kinetics, the LM-OSL intensity is given by

$$L(t) = \gamma\; t\; \Sigma_i\; n0_i\; p_i \left[(b_i - 1)\frac{p_i\; \gamma\; t^2}{2} + 1\right]^{\frac{b_i}{1-b_i}} \tag{5}$$

where b_i is the kinetic order of the ith component peak [2].

In this paper, we present the dependence of the photoionization cross-section of α-Al$_2$O$_3$:C on measurement temperature and the effect of this on other parameters that are related to the photoionization cross-section. Thus, this study represents an effort to characterize point defects involved in the OSL process.

2. Experimental details

All measurements were done using the Risø TL/OSL DA-20 Reader that measures both TL and OSL. The light detection unit consists of an EMI 9235QB photomultiplier tube and a 7-mm thick Hoya U-340 detection filter (transmission 270-380 nm FWHM). The irradiation unit is an in-built ^{90}Sr/^{90}Y β-source with a nominal dose rate of 0.1028 Gy/s. Samples used were aluminium disks measuring 5 mm × 1 mm (Rexon TLD Systems, Ohio, USA). The samples were exposed to 470 nm blue LED light whose stimulation power was linearly increased from 0 to 100% of the maximum stimulation power to produce an LM-OSL signal. The maximum power intensity at the sample position by blue LEDs was 80 mWcm^{-2}. A TL was then measured

at a heating rate of 1 °C/s to record the residual TL signal. All measurements were performed in a nitrogen atmosphere to inhibit spurious luminescence.

Samples were irradiated to 1.0 Gy of β-radiation followed by exposure to blue LEDs for 1000 s. A TL measurement was then taken at 1 °C/s to clear the residual dose i.e. trapped charge 'spared' during optical stimulation. The LM-OSL signal obtained was fitted with equation 1 for $i = 2$. The fitting was perfomed using a "NonlinearModelFit" function in Mathematica which uses the Levenburg-Marquadt algorithm [3] for nonlinear least squares curve-fitting. The goodness of fit was tested by the value of regression squared (R^2).

3. Results and Discussions
3.1. Deconvolution of the LM-OSL signal
Figure 1(a) shows the result of deconvoluting the LM-OSL signal (labelled 1) using equation 1 to produce two components of the LM-OSL peak namely, fast component (labelled 2) and slow component (labelled 3) and Figure 1(b) is a plot of the concomittant residuals. Figure 2(a) is the TL glow-curve before exposing the samples to LEDs and figure 2(b) is the glow-curve obtained due to residual dose after light exposure.
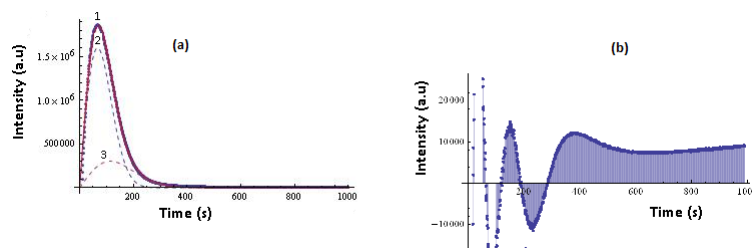

Figure 1. A deconvoluted LM-OSL signal (labelled 1) showing the fast component (labelled 2) and the slow component (labelled 3) (a) and the concomittant residuals (b), $R^2 = 0.9978$. The sample was irradiated to 1.0 Gy and the stimulating power was increased from 0 to 100% at a measurement temperature of 30°C.
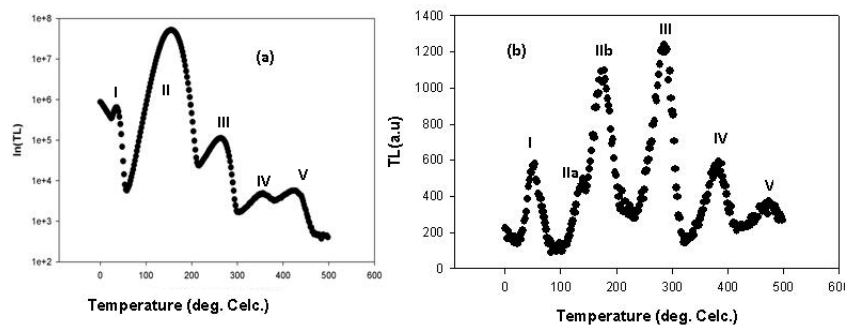

Figure 2. A TL glow curve before exposure to blue LEDs shown on a semi-log scale (a). Residual TL obtained immediately after exposing a sample to blue LEDs (b). The TL was, in each case, measured at 1°C/s after a 1.0 Gy dose.

Peak II in figure 2a is the main peak in α-Al$_2$O$_3$:C that is used for dosimetry applications. It has been reported that peak II is correlated to the LM-OSL peak [5, 6]. Consequently, we

associate the fast OSL component (labelled 2) and the slow OSL component (labelled 3) in figure 1 of the LM-OSL signal to peaks IIa and IIb respectively in figure 2b of the residual TL signal. Considering that the fast component occurs at earlier times than the slow component, it is expected that the photoionization cross-section of the fast component would be larger than that of the slow component. Other researchers [5, 7] fitted the LM-OSL signal with three first-order kinetics components. In our case, fitting with three first-order kinetics components did not yield meaningful parameters' values. The presence of only two first-order components in our investigations can be attributed to either differences in samples used for investigations or the maximum time of sample exposure to blue LEDs since the third component, according to Whitley and McKeever [5] and Dallas et al [7], has its maximum peak position beyond 2000 s whereas the maximum time of 1000 s was used in this study. However, looking at the residual plot, there is a low-intensity persistent signal that does not decay with time, but rather flattens out. This persistent signal could be the third component reported by Whitley and McKeever [5] and Dallas et al [7]. We attribute the fast and slow components obtained in this study to the double-component nature of the TL main peak as seen in figure 2(a). We associate the fast component with easy-to-bleach low temperature component (IIa in figure 2(a)) of the main peak. The slow component which we associate with high temperature component (IIb in figure 2(a)), may be a result of the substantially smaller photoionization cross-section rather than retrapping. We can speculate that the third component as observed by other researchers [5, 7] could be due to OSL from deep traps obtained from direct recombination of stimulated electrons at the luminescence centres or indirectly after retrapping at the main and shallow traps.

3.2. Dependence of photoionization cross-section on measurement temperature
The detrapping probabilities were obtained by fitting the experimental data with equation 1 and the corresponding values of photoionization cross-section were evaluated using equation 2.

Figure 3 shows plots, against measurement temperature, of the detrapping probability (in a) and the photoionization cross-section (in b) for the fast component. Figure 4 shows plots, against measurement temperature, of the detrapping probability (in a) and the photoionization cross-section (in b) for the slow component.
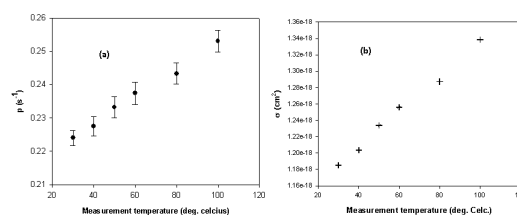

Figure 3. Detrapping probability against measurement temperature for the fast component (a). Photoionization cross-section against measurement temperature for the slow component (b).

Figures 3 and 4, representing the fast component and the slow component respectively, show that both the detrapping probability and the photoionization cross-section increase with measurement temperature. The photoionization cross-section for the fast component increases from 1.1852×10^{-18} cm^{-2} at 30°C to 1.338×10^{-18} cm^{-2} at 100°C representing a 13%increase. As shown in Figure 3, the photoionization increases almost linearly in the temperature range under investigation. On the other hand, the increase in photoionization cross-section for the slow component is nonlinear. The photoionization cross-section for the slow component increases from 4.0529×10^{-19} cm^{-2} at 30°C to 5.225×10^{-19} cm^{-2} at 100°C representing a
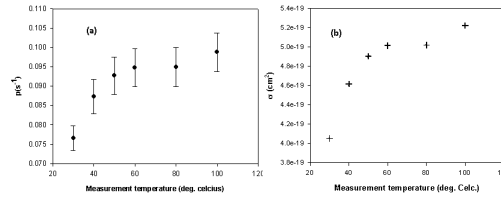
Figure 4. Detrapping probability against measurement temperature for the fast component (a). Photoionization cross-section against measurement temperature for the slow component (b).

29%increase. Whitley and McKeever [5] reported values of $(0.58 - 1.5) \times 10^{-18}$ cm^{-2} for the first component (fast component herein) and $(0.9 - 3.7) \times 10^{-19}$ cm^{-2} for the second component (slow component herein) at a measurement temperature of 70°C, which are consistent with the values reported here. However, Whitley and McKeever [5] used samples obtained from Landauer Inc. (Oklohama, USA) and Bicron NE (Ohio, USA). Furthermore, Whitley and McKeever [5] used a stimulation wavelength of 526nm (green) as compared to 470nm (blue) used in our investigations. The increase in the detrapping probability, which translates into the increase in photoionization cross-section, may be ascribed to a phonon assisted stimulation mechanism.As the measurement temperature increases, electron-phonon interactions become slightly stronger.This affects the detrapping probability and consequently, the photoionization cross-section. The temperature dependence of the electron-phonon interaction can be inferred from the following equation [8]:

$$S = S_0 Coth \left[\frac{\hbar\omega}{kT} \right], \tag{6}$$

where S is the temperature dependent electron-phonon interaction factor ($\gg$ 1 for strong coupling), S_0 is the Huang-Rhys factor at absolute zero, k is the Boltzmann's constant, $\hbar$ is the Planck's constant, T is the absolute temperature, ω is angular frequency, and $\hbar\omega$ is equal to phonon energy. Chruścińska [9], using simulations, also showed that the photoionization cross-section increases with temperature, without considering any particular material.

3.3. Effect of temperature on LM-OSL peak position
Figure 5(a) is a plot of the peak position, t_{max}, against measurement temperature for the fast component whereas figure 5(b) is a similar plot for the slow component. As expected, the peak position moves to earlier times as the measurement temperature increases due to increase in photoionzation cross-section. A large photoionization cross-section ensures that traps are emptied quickly.

Figure 6(a) shows the plot of t_{max} against $1/\sqrt{\sigma}$ for the fast component and figure 6(b) is a similar plot for the slow component. From equation 4, $t_{max} = const/\sqrt{\sigma}$ where $const = \sqrt{T_{stim}/\Phi}$ is the proportinality constant. Thus, a plot of t_{max} against $1/\sqrt{\sigma}$ is expected to produce a straight line with slope *const*. For figure 6(a), $const = 7.22 \times 10^{-8}$ whereas $const = 7.30 \times 10^{-8}$ for figure 6(b) which are consistent. For the values used in this study i.e. $T_{stim} = 1000$s and $\Phi = 1.89 \times 10^{17}$ cm/s, $\sqrt{T_{stim}/\Phi} = 7.27 \times 10^{-8} \approx const$ as expected.

4. Conclusion
The dependence of the photoionization cross-section on measurement temperature in α-Al$_2$O$_3$:C has been investigated. The apparently single LM-OSL peak is a composition of at least two components i.e. the fast and a slow one. The photoionization cross-section of both
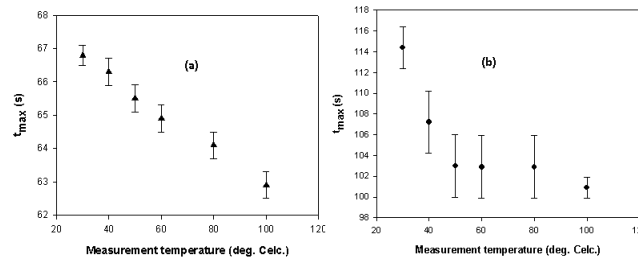
Figure 5. Peak position against measurement temperature for the fast component (a) and a similar plot for the slow component (b).
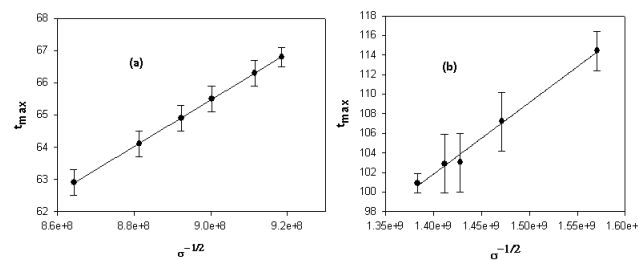

Figure 6. Peak position against the reciprocal of the square root of photoionization cross-section for the fast component (a) and a similar plot for the slow component (b).

components increases with measurement temperature, a behaviour that has been associated with increased electron-phonon coupling as temperature increases. As the measurement temperature is increased, the peak positions shift to earlier times due to increasing photoionization cross-section.

References

[1] Choi, J.H, Duller, G.A.T, Wintle, A.G, 2006 Analysis of Quartz LM-OSL signal Ancient TL **24** (9-20)
[2] Bøtter-Jensen, L, McKeever, S.W.S, Wintle, A.G, 2003 Optically stimulated luminescence dosimetry *Elsevier* (Amsterdam)
[3] Marquadt W.D., 1963 An algorithm for least-squares estimation of nonlinear parameters *J. SOC. INDUST. APPL., MATH* **11** 431-441
[4] Kitis, G, Pagonis, V, 2008 Computerized curve deconvolution analysis for LM-OSL. *Radiat. Meas.* **43** 737-41
[5] Whitley, V.H and McKeever, S.W.S, 2002 Linear modulation optically stimulated luminescence and thermoluminescence techniques in Al_2O_3:C. *Radiat. Prot. Dos.* **100** (61-6)
[6] Walker, F.D, Colyott, E, Agersnap Larsen, N, McKeever, S.W.S, 1996 The wavelength dependence of light-induced fading of TL from α-Al_2O_3:C *Radiat. Meas.* **26** (711-8)
[7] Dallas, G.I, Polymeris, G.S, Stefanaki, E.C, Afouxenidis, D, Tsirliganis, N.C, Kitis, G, 2008 Sample dependent correlation between TL and LM-OSL in Al_2O_3:C *Radiat. Meas.* **43** (335-40)
[8] Hayes, W., Stoneham, A.M., 1985, Defects and defect processes in nonmetallic solids *John Wiley and Sons, New York*
[9] Chruścińska A, 2010. On some fundamental features of optically stimulated luminescence measurements *Radiat. Meas.* **45** (991-9)